

C IV fluxes from the Sun as a star, and the correlation with magnetic flux

C.J. Schrijver (P.I.), J.L. Linsky (Co-P.I.), J. Bennett, A. Brown, S.H. Saar

P.I. Institution: Joint Institute for Laboratory Astrophysics, University of Colorado and National Bureau of Standards, Campus Box 0440, Boulder, CO 80309-0440, U.S.A.

NASA grant number: NAG5-932

UCB account number: 153-1213

A total of 144 C IV $\lambda 1548$ SMM-UVSP spectroheliograms of solar plages have been analyzed, some of which are series of exposures of the same region on the same day. We also analyzed C IV $\lambda 1551$ rasters of plages and C IV $\lambda 1548$ rasters of the quiet Sun. The sample contains data on 17 different plages, observed on 50 different days. The center-to-limb variations of the active regions show that the optical thickness effects in the C IV $\lambda 1548$ line can be neglected in the conversion from intensity to flux density (as was previously shown for quiet regions). As expected for the nearly optically thin situation, the C IV $\lambda 1548$ line is twice as bright as the C IV $\lambda 1551$ line. The average C IV $\lambda 1548$ flux density (derived from count rates in two adjacent 0.3 Å slits, and corrected for the estimated part of the line flux outside the 0.6 Å total window) for a quiet region is $2.7 \cdot 10^8 \text{ erg cm}^{-2} \text{ s}^{-1}$ and, with surprisingly little scatter, $1.8 \cdot 10^8 \text{ erg cm}^{-2} \text{ s}^{-1}$ for plages.

The intensity histograms of rasters obtained at disk center can be separated into characteristic plage and quiet-Sun contributions with variable relative filling factors.

The disk-averaged flux density ($F_{CIV,d}$) in the C IV doublet (observed with the Solar Mesosphere Explorer) and the disk-averaged magnitude of the magnetic flux density ($| \langle fB \rangle |$) (derived from synoptic magnetic maps produced at Kitt Peak National Observatory) are related through:

$$\langle F_{CIV,d} \rangle = 2.2 \cdot 10^8 \times (| \langle fB \rangle |)^{0.8}.$$

The relationship between the C IV and magnetic flux densities for spatially resolved data is inferred to be almost the same, with only an additional factor of order unity in the constant of proportionality.

A publication is in preparation.

(NASA-CR-183156) C 4 FLUXES FROM THE SUN AS
A STAR AND THE CORRELATION WITH MAGNETIC
FLUX Final Report (Joint Inst. for Lab.
Astrophysics) 13 p
CSCL 03B

G3/92
0157042
Unclas

N89-10627

30 August 1988

Final report

157042
11-10-92
9000-10-92

1 Introduction

The study of stellar magnetic activity can benefit greatly from the combination of solar and stellar data: Stellar observations provide insight in the total energy budget of stellar outer atmospheres as a function of basic stellar parameters such as effective temperature, gravity and rotation rate. Observations of atmospheric radiative losses in a series of diagnostics can even tell us something about the heating processes, but understanding the physical processes of energy transport, dissipation and redistribution requires knowledge of the topology of the magnetic field. This detailed knowledge of the outer stellar atmosphere can currently be obtained only through study of spatially resolved observations of the nearest example of a magnetically active star: the Sun.

Only a few radiative diagnostics are available that have been studied both for solar-type stars and for the spatially-resolved Sun: Observations of Ca II H+K fluxes have been obtained for the Sun with, for instance, the KPNO-McMath (Schrijver et al. 1983) and for stars at Mt. Wilson. The chromospheric C II (1335Å) line has been observed by the *International Ultraviolet Explorer* (IUE) for a large number of cool stars, and by the *Skylab Apollo Telescope Mount* (ATM) for solar active and quiet regions. The X-ray emission from solar quiet and active regions were also measured by instruments on the ATM; the stellar counterpart of these X-ray observations were performed with the *HEAO-2 EINSTEIN* and *EXOSAT* satellites. The current investigation increases the overlap in stellar and solar data by adding the important transition-region doublet of C IV near 1550Å to the list. The formation temperature of the C IV lines is approximately 100,000 Kelvin, whereas the hottest non-coronal diagnostic for both stellar and solar activity to date, the C II line, has a formation temperature of some 20,000 K. Hence the C IV line provides new information at a temperature significantly separated from both chromospheric and coronal temperatures. The emission in the C IV doublet from stars is observed by IUE and for the spatially resolved Sun by, for instance, the *Solar Maximum Mission* Ultraviolet Spectrometer and Polarimeter (UVSP) experiment.

The current investigation, which uses solar C IV spectroheliograms obtained with the UVSP, has several goals: a) we determine typical mean C IV intensities for quiet regions and for plages, yielding the extremes of ordinary solar activity, b) we determine the center-to-limb effects in the C IV lines which can be used in the modelling of rotational modulation of stellar data observed with satellites such as IUE, c) we establish the relationship between the C IV intensity and the magnetic flux density for the Sun observed as a star, and derive the relationship for spatially resolved data.

2 Selection and calibration of SMM-UVSP spectroheliograms

The SMM-UVSP is described in detail by Woodgate et al. (1980). The UVSP spectrometer can

be used in a mode in which two adjacent detectors (# 3 and #4) observe one of the lines in the C IV doublet around 1550Å. An image of a solar region can be constructed by moving the secondary mirror, thus displacing the solar image across an entrance slit.

We selected UVSP rasters from all C IV $\lambda 1548$ and $\lambda 1551$ rasters obtained between March and October of 1980. Rasters were selected for which detectors #3 and #4 were used to observe one of the two C IV lines. The selected rasters contained 80x30 pixels and were obtained using the 3x3 arcsec entrance slit with an integration time of 0.063 sec. per pixel. Rasters were rejected if they showed major data gaps or errors when visually inspected, and if major flares occurred at the time of exposure. This yielded a total of 144 C IV $\lambda 1548$ rasters of plages. Due to a pointing offset of the UVSP generally only the north-west corner of the plages is seen.

Only one of the lines of the C IV doublet is observed at any one time. We concentrate on the 1548Å line, but also include results for the 1551Å line. The lines are observed in two adjacent 0.3Å windows (the red and blue windows). We apply a correction factor of 1.6 for different detector responses, see Gurman and Athay (1983). We use the average ratio of the blue to the red channel for the entire raster to obtain information on the slit position relative to the line (time dependent, for instance, owing to orbital Doppler shift). With this information and by assuming a mean FWHM line width of 0.25Å (e.g. Athay and White, 1980) the observed count rates can be corrected to yield to total count rate for the entire spectral line. The count rate corrections are smaller than approximately 5% for all rasters. Count rates are converted to intensities by using a factor of 17.6 erg cm⁻² s⁻¹ (Woodgate et al., 1980; Gurman and Athay, 1983).

3 C IV intensities in the quiet Sun and in plages

a) The quiet Sun

We determined the distribution function $g_q(I_{1548})$ for a typical quiet region on the Sun by using six rasters obtained at disk center of particularly quiet regions (Table 1). The distribution function shown in Figure 1 closely resembles that derived by Gurman (1983) who used a much larger data set. The average C IV $\lambda 1548$ intensity is $I_{1548,q} = 870$ erg cm⁻² s⁻¹ sr⁻¹ (in good agreement with the value of 844 erg cm⁻² s⁻¹ sr⁻¹ given by Gurman, 1983). The 1- σ spread in intensities derived from g_q is 850 erg cm⁻² s⁻¹ sr⁻¹. This average intensity for quiet regions corresponds to a flux density of $F_{C IV,q} = 4.1 \cdot 10^3$ erg cm⁻² s⁻¹ in the $\lambda 1548, 1551$ doublet, if optical thickness effects are negligible (so that the intensity in the C IV $\lambda 1548$ line is twice that of the C IV $\lambda 1551$ line, and $F = \pi I$). This flux level is comparable to the lowest detections of IUE (which, in low-resolution mode, can observe only the total flux in the doublet) of stars of spectral type similar to that of the Sun (e.g. Schrijver 1987a).

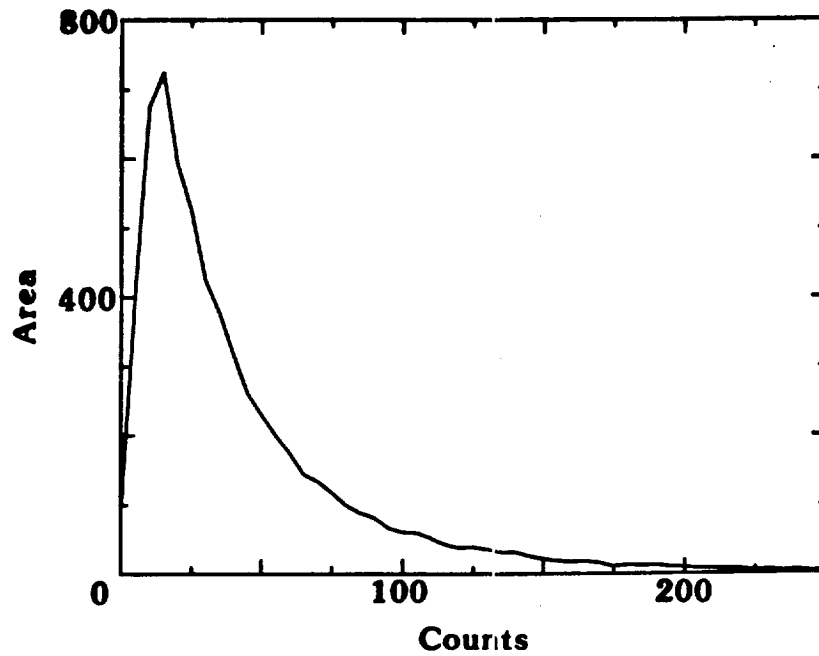


Figure 1. Mean distribution function of C IV $\lambda 1548$ intensities, g_p , in the quiet Sun, as determined from six observations at disk center (see Table 1).

Very cool giant stars have been observed with flux levels as low as $100 \text{ erg cm}^{-2} \text{ s}^{-1}$. In both cases the observed fluxes are close to the instrumental detection limit.

Table 1. List of observations of quiet regions near disk center used to determine a mean intensity distribution function for the C IV $\lambda 1548$ line. Entered are the UVSP exposure number, the date of observation, and the fractional distance ρ from disk center.

Exposure number	Date (1980)	ρ
2707	10 May	0.07
2739	12 May	0.09
2875	14 May	0.09
4325	14 Jun	0.07
7418	3 Aug	0.08
12238	25 Sep	0.11

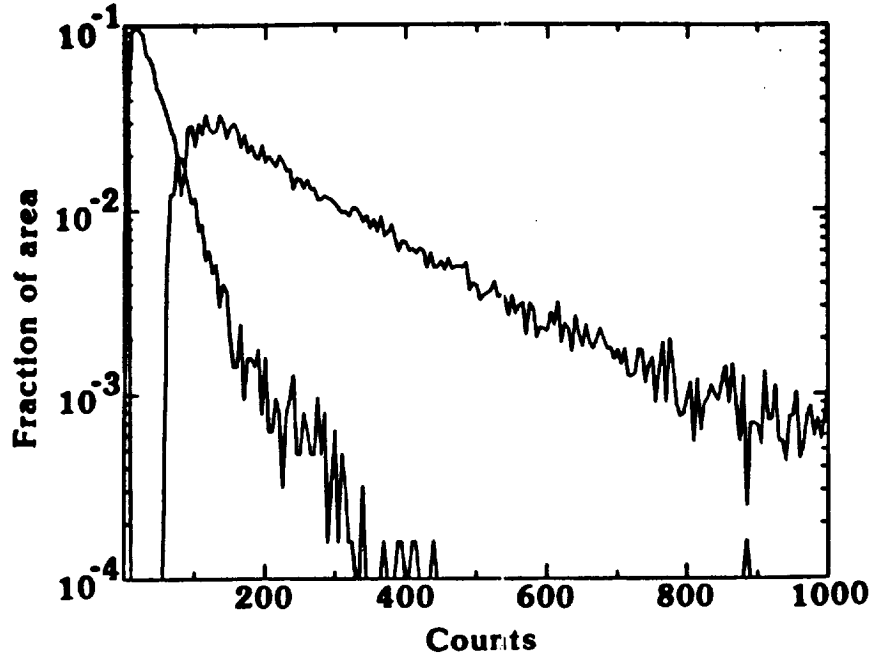


Figure 2. Mean distribution function g_p of C IV $\lambda 1548$ intensities in plages, derived from observations listed in Table 2, compared with the distribution function g_q for the quiet Sun (also in Fig. 1).

b) The plage component

Once the distribution g_q of intensities is determined for a typical quiet region, a distribution g_p of intensities associated with plages can be determined. Such a separation may not be practical for the Sun as a whole, since the diffusion of flux across the solar surface affects all regions in some fashion (see Schrijver and Harvey, 1988, for a discussion). The separation may be useful for small fields of view surrounding plages because in that case mostly the inner plage regions are studied which are relatively isolated from the surroundings (see Schrijver 1988).

We first determine the distribution of C IV $\lambda 1548$ intensities for nine active-region observations (Table 2). The quiet-region component is then subtracted by normalising the quiet-region histogram assuming that every pixel with an intensity less than 50 counts per gate time (0.063 sec), i.e. the average intensity $I_{1548,q}$ for a quiet region, is effectively "quiet". Figure 2 compares the mean plage intensity distribution with that for the quiet Sun.

4 Optical thickness effects

For the current investigation we are not interested in a determination of the optical thickness of the C IV lines, but merely wish to establish whether the optical thickness plays an appreciable role in the

Table 2. *List of observations used to determine the characteristic distribution function of C IV $\lambda 1548$ intensities of plages. Listed are the Boulder active-region number, the UVSP exposure number, the observation date, the fractional distance ρ from disk center, and I_{1548} ($\text{erg cm}^{-2} \text{ s}^{-1} \text{ sr}^{-1}$).*

Region number	Exposure number	Date (1980)	ρ	I_{1548} (*10 ³)
2351	765	27 Mar	0.50	6.1
2396	1873	21 Apr	0.47	10.1
2411	2139	29 Apr	0.43	7.7
2418	2317	4 May	0.37	6.7
2456	3028	18 May	0.50	6.7
2490	3900	7 Jun	0.40	6.2
2502	4258	13 Jun	0.37	7.6
2517	4731	20 Jun	0.39	5.7
2646	11036	1 Sep	0.27	7.0

conversion of the observed line intensities to flux densities. An appreciable optical thickness in the C IV lines would show up a) as a ratio in the C IV $\lambda 1548$ and C IV $\lambda 1551$ line intensities different from two, and b) as a limb-brightening curve for the specific intensity that would differ from the expected change due to projection effects only.

Figure 3 compares the average distribution functions of four pairs of observations of active regions: pairs of C IV $\lambda 1548$ and C IV $\lambda 1551$ rasters were selected that were obtained of plages near disk center, with little or no changes in pointing between the two exposures and obtained with at most 1.5 hrs between the two spectral line settings. The intensities in the C IV $\lambda 1551$ line were scaled up by a factor of two to obtain the histogram displayed in Figure 3. The agreement of the two curves suggests that optical thickness effects are small.

In order to determine the center-to-limb effects for plages in the SMM-UVSP C IV data we used a method similar to that used by Schrijver et al. (1985). The center-to-limb effects are determined for active regions as a whole: the average specific intensity of active regions is plotted against the fractional distance from disk center. The average specific intensity is derived by averaging the count rates for all pixels above a threshold level. This threshold, defining the perimeter of the active region, was defined by

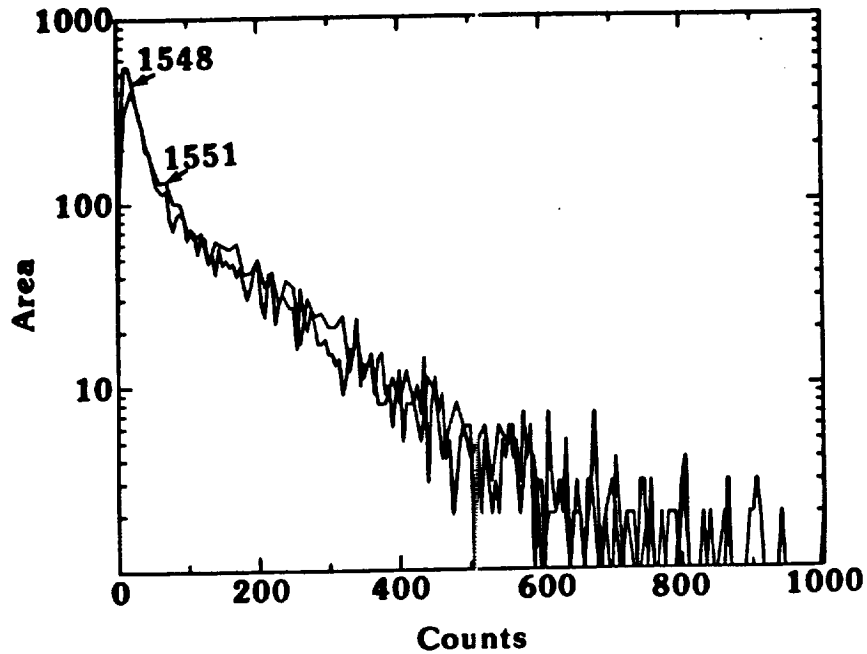


Figure 3. Comparison of the distribution of intensities in the C IV $\lambda 1548$ and C IV $\lambda 1551$ lines. The average distribution functions were obtained from four sets of two rasters of plages and surroundings. The intensities for the C IV $\lambda 1551$ line were scaled up by a factor of two.

Schrijver *et al.* (1985) using an analysis of distribution functions of specific intensities. This threshold level corresponds to an average magnetic flux of approximately 50 Gauss as observed in the Fe I 5233Å line (Schrijver 1987b).

Schrijver *et al.* (1985) used the characteristic shape of the distribution function of intensities of quiet regions to define a boundary intensity for active regions: they used a threshold intensity of $\langle I \rangle + 1.5 \times \sigma$. If one uses the fact that the C IV $\lambda 1548$ line in quiet regions can be regarded as essentially optically thin, one can correct the threshold intensity for different positions on the disk. Figure 4 shows the mean plage intensity in the C IV $\lambda 1548$ line versus the fractional distance from Sun center. The limb brightening is virtually equal to the limb brightening expected for an optically thin line, except for the regions very near the limb. Optical thickness effects and the crudeness of the use of a fixed threshold intensity may both play a role near the solar limb.

Correction for the center-to-limb effects yields a mean C IV $\lambda 1548$ intensity for plages of 5.9×10^3 erg cm⁻² s⁻¹ sr⁻¹. The data suggest that optical thickness effects can indeed be neglected in the conversion of intensities to flux densities (see also, for instance, Athay and White, 1980, Athay *et al.*

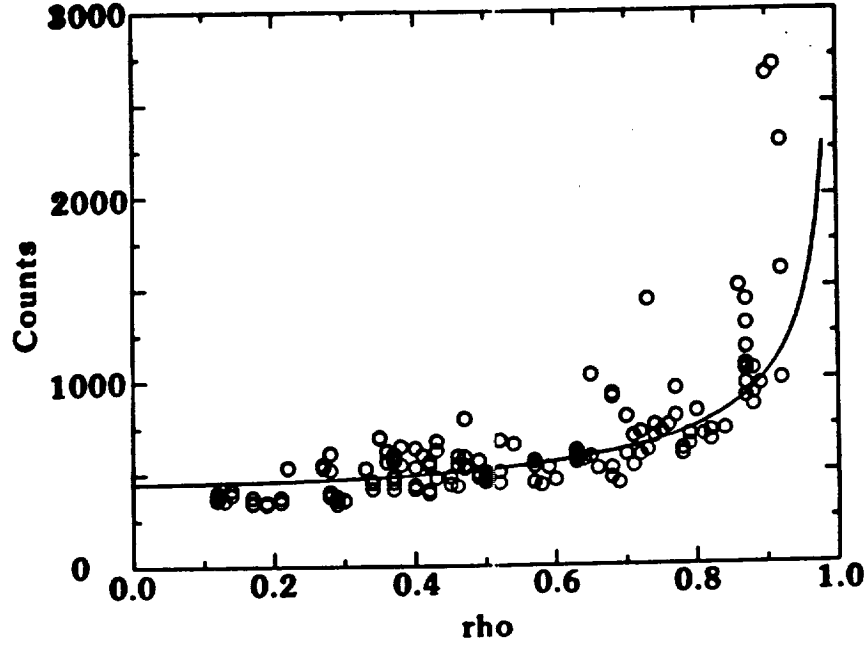


Figure 4. Specific intensity of plages (in counts per gate time) vs. fractional distance from disk center. The curve represents the limb brightening expected in the case of an optically thin line due to projection effects.

1983), and that the ratio of C IV $\lambda 1548$ to C IV $\lambda 1551$ is indeed 2:1 as expected in the optically thin case, so that the mean plage flux density for the C IV doublet is $2.8 \cdot 10^4 \text{ erg cm}^{-2} \text{ s}^{-1}$. Stars are observed with C IV $\lambda 1548 + 1551$ flux densities in excess of $10^6 \text{ erg cm}^{-2} \text{ s}^{-1}$ (e.g. Schrijver 1987a).

The fact that the C IV lines behave as optically thin lines can be used in the study of rotational modulation curves observed for magnetically active stars, for instance by comparing modulation curves in different activity diagnostics with different centre-to-limb variations.

5 The relationship between of $F_{C IV}$ and $|\langle fB \rangle|$

a) The Sun-as-a-star:

We now turn to the relationship between the flux density in the C IV doublet and the magnetic flux density. We first study this relationship as observed for the Sun as a star. Figure 5 relates the average flux density in the C IV doublet for six month intervals as observed with the Solar Mesosphere Explorer (Mount and Rottman, 1985) with the average magnetic flux density derived from synoptic magnetic maps produced at Kitt Peak National Observatory (see Table 3). The best-fit relation (assuming equal relative errors in both axes) is

$$\langle F_{C IV, d} \rangle = 2.2 \cdot 10^3 \times \langle |\langle fB \rangle| \rangle^{0.5}. \quad (1)$$

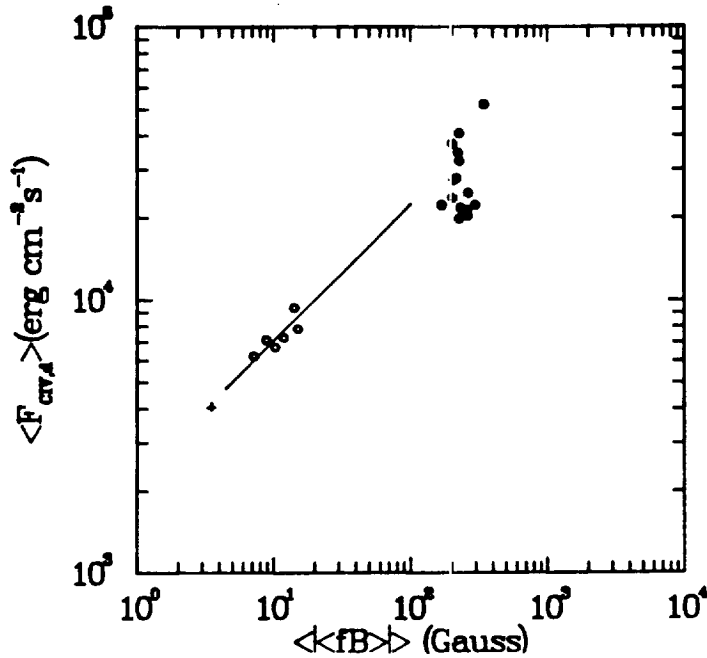


Figure 5. Relationship between the hemisphere-averaged flux density $F_{C\,IV,4}$ in the C IV $\lambda\,1548 + 1551$ doublet, as observed by the SME, and the hemisphere-averaged magnetic flux density, as derived from synoptic magnetograms, both averaged over six solar rotations (open circles, see Table 3). The line represents Eq. 1. Also shown are the data for the quiet Sun (+) and for active regions near disk center (filled circles, see Table 4).

b) Spatially resolved data

If one knows the relation between radiative and magnetic flux densities, the relation for spatially resolved data can in principle be derived from that relation, provided that the distribution function of magnetic fluxes over the solar surface throughout the solar cycle is known. Schrijver and Harvey (1988) study how the time-dependent distribution function h_i of magnetic flux over the solar surface transforms relations between a radiative diagnostic and the mean magnetic flux density, both obtained from spatially resolved data, into relations between these quantities for disk-integrated observations at different times in the solar activity cycle. They assume a power-law relation between any radiative diagnostic of activity (expressed as a flux density F_i) and the magnetic flux density (on a scale that smoothes out small-scale temporal and spatial fluctuations):

$$F_i = a_i |\langle fB \rangle|^{b_i}. \quad (2)$$

Table 3. List of hemisphere-averaged magnetic flux densities $\langle |fB| \rangle$ (averages over six solar rotations, as derived from synoptic magnetograms obtained in the 8688Å line, see Schrijver and Harvey 1988) and C IV $\lambda 1548 + 1551$ flux densities $F_{C\ IV,\lambda}$ (erg cm⁻² s⁻¹) as observed by the Solar Mesosphere Explorer (from Bennett 1987) averaged over the same six month intervals.

Mean date	Solar rotation numbers	$\langle fB \rangle$ (Gauss)	$F_{C\ IV,\lambda}$ (*10 ³)
1982.2	1717-1722	14.2	9.4
1982.7	1723-1728	15.1	7.8
1983.1	1729-1734	11.9	7.3
1983.6	1735-1740	10.3	6.7
1984.0	1741-1746	8.9	7.1
1984.5	1747-1752	7.2	6.2

The disk-averaged magnetic flux density $\langle |fB| \rangle$ is given by:

$$\langle |fB| \rangle_t = \int_0^{|fB|_{\max}} |fB| h_t d|fB|, \quad (3a)$$

where $|fB|_{\max}$ is the maximal flux density that is included in the computation. The introduction of $|fB|_{\max}$ is required by the physics of the problem: since we intend to use the distribution functions to compute disk-averaged radiative fluxes, and the intensities over spots in many activity diagnostics are markedly reduced as compared to the intensities over surrounding regions (Webb and Zirin 1981) the convolution of Eq. (3a) should not include spots.

The calculation of the disk-averaged radiative flux density $\langle F_i \rangle$ requires the following integration:

$$\langle F_i \rangle_t = \int_0^{|fB|_{\max}} a_i |fB|^{b_i} h_t d|fB|. \quad (3b)$$

By performing the integrations (3a,b) at different times t in the solar cycle one obtains the relation between the disk-averaged radiative flux density $\langle F_i \rangle_t$ and magnetic flux density $\langle |fB| \rangle_t$ for the Sun as it changes its level of activity throughout the cycle.

Schrijver and Harvey (1988) show that the relations between $\langle F_i \rangle_t$ and $\langle |fB| \rangle_t$ can be described

accurately by power-law fits:

$$\langle F_i \rangle_t = \alpha_i 2.5^{b_i(b_i-1)} \langle |fB| \rangle_t^{b_i}. \quad (4)$$

If $b_i = 0.5$ (as is the case for the relation between the flux density in the C IV doublet and the magnetic flux density, see Eq. 1): $2.5^{b_i(b_i-1)} = 0.80$. Hence the relations between the C IV and magnetic flux densities for spatially resolved data and disk-integrated data are expected to be very similar, as is indeed witnessed by the fact that the data for plagues † and the quiet Sun lie very near the relation for disk-averaged data in Figure 5 (cf. Table 4). Keeping in mind the intercalibration uncertainties between the SME and the SMM-UVSP, the agreement with the expected nature of the relations is indeed very good.

These results for the C IV doublet can be indirectly related with other diagnostics through other relations between radiative and magnetic diagnostics (e.g. Schrijver *et al.* 1988).

We did not attempt to establish a point by point correlation between the C IV intensity and the magnetic flux density, which would require complicated transformations and alignments between two data sets that were not simultaneously obtained and do not have the same spatial resolution. We can, however, use the distribution functions that were obtained in Section 3 to verify whether Equation 1, relating C IV and magnetic flux densities through a power law with index 0.5, is consistent with the observed distribution functions. This way one does not need to correlate the data point by point.

A major portion of the distribution function for plagues can be approximated by a power-law fit (compare Fig. 2):

$$g_p(I) dI = \alpha \times 10^{-\beta I} dI. \quad (5)$$

Table 4 lists slopes β for plague observations obtained near disk center.

If the intensity I and the magnetic flux density $|fB|$ are related through:

$$I = \gamma \times \sqrt{|fB|}, \quad (6)$$

then the distribution function for the magnetic flux density should be:

$$f(|fB|) d|fB| = \frac{\alpha\gamma}{\sqrt{|fB|}} \times 10^{-\beta\gamma\sqrt{|fB|}} d|fB|. \quad (7)$$

† Note that the mean magnetic flux densities for plagues listed here are approximately twice as large as the values found by Schrijver (1987b). This may be related with the use of another spectral line to measure the fields (J.W. Harvey, private communication). Locating the cause of the difference is currently under investigation). The two sets of magnetic data entered into Figure 5 and listed in Table 4 have been observed with the same diagnostic.

Table 4. List of mean magnetic flux densities $| \langle fB \rangle |$ (with observation dates) and average C IV $\lambda 1548$ intensity I_{1548} ($\text{erg cm}^{-2} \text{ s}^{-1}$) of 15 active regions (specified by their Boulder number) when nearest to disk center (listed are also the corresponding fractional distance ρ from disk center and observation date). In five cases averages for multiple rasters are given. In six cases (for which $\rho < 0.5$) the slope β of a linear fit to $\log g_p$ is given (cf. Eq. 5).

A.R. Number	$ \langle fB \rangle $ (Gauss)	Date (1980)	Mean C IV intensity (*10 ³)	Slope β of $\log g_p(I_{1548})$ (*10 ⁻⁴)	No. of exposures	ρ	Date (1980)
2363	174	1 Apr	5.8		5	0.64	1 Apr
2391	194	16 Apr	4.9		1	0.78	19 Apr
2396	173	23 Apr	9.2		1	0.47	21 Apr
2411	296	2 May	12.8		1	0.73	27 Apr
2418	177	5 May	6.7	-1.27	5	0.25	5 May
2456	224	20 May	5.0	-1.72	1	0.14	19 May
2470	221	25 May	5.2		1	0.79	29 May
2490	254	8 Jun	5.5	-1.22	5	0.37	8 Jun
2502	190	14 Jun	8.5	-1.33	1	0.35	14 Jun
2517	199	21 Jun	5.3	-1.95	3	0.39	20 Jun
2522	194	22 Jun	7.9		1	0.77	26 Jun
2611	145	14 Aug	5.5		2	0.89	10 Aug
2629	194	20 Aug	10.0		1	0.86	25 Aug
2645	226	2 Sep	6.0		1	0.54	31 Aug
2646	185	2 Sep	6.9	-1.33	1	0.27	1 Sep

This is indeed consistent with observed distribution functions for the magnetic flux density within plages.

6 Summary of conclusions

- 1 The C IV lines at 1548Å and 1551Å can be regarded to be optically thin in the conversion of intensities to flux densities, both in quiet regions and in plages. This result can be used to compare solar and stellar C IV fluxes and to interpret stellar rotational modulation curves for the C IV doublet.

2 The average C IV $\lambda 1548$ flux density, $F_{C\ IV}$, of a typical quiet region on the Sun is $2.7 \cdot 10^3$ erg cm⁻² s⁻¹.

3 If the field of view is small enough as compared to the plage, a distribution function g_p can be derived for I_{1548} that is characteristic of the central parts of active regions in general (see Fig. 2).

4 Related with the existence of a characteristic distribution function g_p for I_{1548} is the fact that the average flux density for plages in C IV $\lambda 1548$ shows little scatter around the value of $1.8 \cdot 10^4$ erg cm⁻² s⁻¹.

5 The relationship for stellar, hemisphere averaged data $\langle F_{C\ IV} \rangle = 2.2 \cdot 10^3 \langle |fB| \rangle$, and is inferred to be $F_{C\ IV} = 3.1 \cdot 10^3 |fB|$ for spatially resolved data (with a resolution of approximately 10 arcsec).

Acknowledgements

CJS gratefully acknowledges the hospitality of A. M. Title and his group at the Lockheed Palo Alto Research Laboratory, and of the National Solar Observatories at Tucson. He thanks S. Ferguson, K.L. Harvey, and R. Shine for their help in the data reduction.

References

- Athay, R.G., White, O.R. 1980, *Astrophys. J.* 240, 306
- Athay, R.G., Gurman, J.B., Henze, W., Shine, R.A. 1983, *Astrophys. J.* 265, 519.
- Bennett, J.O. 1987, Ph. D. Thesis, University of Colorado.
- Gurman, J.B. 1983, "A Study of C IV Intensity Distributions in the Quiet Sun from UVSP Data," Applied Research and Systems Report.
- Gurman J.B. , Athay, R.G. 1983, *Astrophys. J.* 273, 374.
- Mount, G.H., Rottman, G.J. 1985, *J. Geophys. Res.* 90, 13031.
- Schrijver, C.J. 1987a, in "Cool Stars, Stellar Systems, and the Sun, J.L. Linsky and R.E. Stencel (eds.), Springer-Verlag, p 135.
- Schrijver, C.J. 1987b, *Astron. Astrophys.*, 180, 241.
- Schrijver, C.J. 1988, submitted to *Solar Physics*.
- Schrijver, C.J., Coté, J., Zwaan, C., Saar, S.H. 1988, *Astrophys. J.*, in press.
- Schrijver, C.J., Harvey, K.L.: 1988, to be submitted to *Astrophys. J.*
- Schrijver, C.J., Zwaan, C., Maxson, C.W., Noyes, R.W. 1985, *Astron. Astrophys.* 149, 123.
- Webb, D.F., Zirin, H. 1981, *Solar Phys.* 69, 99.
- Woodgate, B.E. et al. 1980, *Solar Physics* 65, 73.